PAPER

Check for updates

A sensitive fluorescent probe for the polar solvation dynamics at protein–surfactant interfaces†

Priya Singh,[a] Susobhan Choudhury,[a] Subhankar Singha,[b] Yongwoong Jun,[b] Sandipan Chakraborty,[c] Jhimli Sengupta,[d] Ranjan Das, [ID] *[d] Kyo-Han Ahn[b] and Samir Kumar Pal [ID] *[a]

Relaxation dynamics at the surface of biologically important macromolecules is important taking into account their functionality in molecular recognition. Over the years it has been shown that the solvation dynamics of a fluorescent probe at biomolecular surfaces and interfaces account for the relaxation dynamics of polar residues and associated water molecules. However, the sensitivity of the dynamics depends largely on the localization and exposure of the probe. For noncovalent fluorescent probes, localization at the region of interest in addition to surface exposure is an added challenge compared to the covalently attached probes at the biological interfaces. Here we have used a synthesized donor–acceptor type dipolar fluorophore, 6-acetyl-(2-((4-hydroxycyclohexyl)(methyl)amino)naphthalene) (ACYMAN), for the investigation of the solvation dynamics of a model protein–surfactant interface. A significant structural rearrangement of a model histone protein (H1) upon interaction with anionic surfactant sodium dodecyl sulphate (SDS) as revealed from the circular dichroism (CD) studies is nicely corroborated in the solvation dynamics of the probe at the interface. The polarization gated fluorescence anisotropy of the probe compared to that at the SDS micellar surface clearly reveals the localization of the probe at the protein–surfactant interface. We have also compared the sensitivity of ACYMAN with other solvation probes including coumarin 500 (C500) and 4-(dicyanomethylene)-2-methyl-6-(*p*-dimethylamino-styryl)-4*H*-pyran (DCM). In comparison to ACYMAN, both C500 and DCM fail to probe the interfacial solvation dynamics of a model protein–surfactant interface. While C500 is found to be delocalized from the protein–surfactant interface, DCM becomes destabilized upon the formation of the interface (protein–surfactant complex). The timescales obtained from this novel probe have also been compared with other femtosecond resolved studies and molecular dynamics simulations.

1. Introduction

Understanding complex phenomena emerging as a result of multi-scale dynamic biological interactions is one of the major challenges in contemporary biology.[1–3] Solvation dynamics is a powerful technique for the quantification of relaxation phenomena of biological macromolecules and has found increasing use in the study of biomolecular surfaces and interfaces.[4–10]

In a typical solvation dynamics experiment the relaxation of a fluorophore is carefully monitored following photoexcitation by a femtosecond/picosecond laser pulse.[11,12] For an ideal fluorophore with less complicated excited state events, the relaxation dynamics is essentially governed by the solvent molecules in the immediate vicinity of the probe.[13] In the case of a fluorophore covalently attached to the biological macromolecules surface exposure is found to be an issue for the investigation of the relaxation dynamics.[14] This issue becomes more vital in the case of interfacial relaxation dynamics of a biological macromolecule in contact with other biological and biomimetic surfaces. While indigenous fluorophores (fluorescent amino acids in proteins and bases in DNA) suffer from complicated excited state photo-physics, attachment of extrinsic probes may perturb the local structure of biomolecules.[15,16] Sometimes non-covalently bound fluorophores become very effective in the investigation of biological surfaces, because of
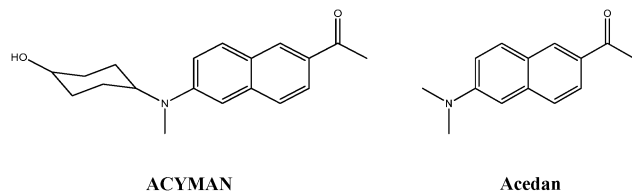
[a] Department of Chemical, Biological & Macromolecular Sciences, S. N. Bose National Centre for Basic Sciences, Block JD, Sector III, Salt Lake, Kolkata 700 106, India. E-mail: skpal@bose.res.in

[b] Department of Chemistry, Pohang University of Science and Technology (POSTECH), 77 Cheongam-Ro, Nam-Gu, Pohang, Gyungbuk, 790 784, Republic of Korea

[c] Department of Physical Chemistry, IACS, Jadavpur, Kolkata 700032, India

[d] Department of Chemistry, West Bengal State University, Barasat, Kolkata 700126, India. E-mail: ranjan.das68@gmail.com

† Electronic supplementary information (ESI) available. See DOI: 10.1039/c6cp08804j

This journal is © the Owner Societies 2017

Phys. Chem. Chem. Phys., 2017, **19**, 12237–12245 | 12237

Scheme 1 Structures of ACYMAN (left) and acedan (right).

their selective attachment being governed by specific physical forces which includes Coulombic, hydrophobic or dipolar interaction.[17] But, for obvious reasons, a non-covalent solvation probe for the surface of a biomolecule may not be useful for the investigation of the interface of the biomolecule with another biological or biomimetic surface. For example, in one study, electrostatically bound 2-(p-toluidino)naphthalene-6-sulfonate (TNS) was used to investigate the surface polarity of the Histone 1 (H1) protein, which is found to be displaced to bulk water upon complexation of the protein with genomic DNA.[18] Thus the investigation of the surface and interface of a biological macromolecule using a non-covalently bound fluorophore is quite challenging and such reports are sparse in the literature.

Here, we have synthesized a fluorescent probe, 6-acetyl-(2-((4-hydroxycyclohexyl)(methyl)amino)naphthalene) (ACYMAN), which is a derivative of acedan[19] (Scheme 1) for the investigation of a biological interface. ACYMAN is moderately polar in the ground state (ground state dipole moment ~ 2.0 D); however, upon UV excitation, it undergoes an intramolecular charge transfer (ICT) reaction to become highly polar in the excited state (excited state dipole moment ~ 7.1 D) and it is known to display solvent-polarity sensitive fluorescence similar to acedan.[19] The dye (ACYMAN) has a moderate fluorescence quantum yield in water (10%), and possesses good solubility in water ($\sim 10^{-4}$ M) which makes it suitable for studying protein–water interfaces. For the present study, we have taken the interface of a nuclear protein H1 (cationic) and an anionic surfactant (SDS) as a model system for the investigation of interfacial solvation dynamics and compared the same with that at the micellar surface. The H1–SDS (much below the critical micellar concentration (CMC) of the anionic surfactant) system under investigation is also biologically important as the interaction with the anionic SDS monomers induces a helical structure in the H1 protein as evidenced from our CD studies. Such observation of induction of the helix structure in the protein upon electrostatic interaction with DNA has been reported,[20,21] which is concluded to be one of the key factors in chromatin condensation.[4,22] While the dynamics of hydration at the surface of H1 is reported to be ultrafast[18] (up to a few picoseconds) in nature, the interfacial dynamics upon the formation of an electrostatically driven interface is sparse in the literature. One of the earlier studies concluded that the interfacial dynamics at the junction of a H1–DNA complex is not much different from that of the protein surface itself.[18] However, this femtosecond resolved experiment was performed with a covalently labeled dansyl probe inviting the possibility of local structural perturbation in addition to losing information on the slower dynamics of structurally ordered water (SOW) molecules,

which are relevant to the structural transition of the biomolecule.[23] We have used the noncovalent novel fluorescent dye ACYMAN to probe the H1–SDS interface, especially the SOW and associated environmental dynamics upon structural transition from random coil to α-helix with picosecond resolution in an experimental window of several nanoseconds. We have also compared the dynamics with those at the surface of the H1 protein and micelles formed by the SDS monomers. The geometrical restriction of the dye in the microenvironments has been explored from polarization gated fluorescence studies. In order to establish the efficacy of ACYMAN in the exploration of interfacial solvation dynamics, we have compared the dynamics with other commercially available fluorescent reporters (dyes).

2. Materials and methods

Chemicals

The histone from calf thymus (type III-SS) (H1) and sodium dodecyl sulfate (SDS) were purchased from Sigma (Saint Louis, USA). All the aqueous biological solutions were prepared in phosphate buffer (50 mM, pH 7). The experimental procedure for the synthesis of the ACYMAN dye has been described earlier.[19]

Experimental details

The steady state emission spectra were measured with a Jobin Yvon Fluorolog fluorimeter. All the picosecond resolved fluorescence transients were measured by using a commercially available time-correlated single-photon counting (TCSPC) setup with MCP-PMT from Edinburgh instruments, U.K. (instrument response function (IRF) of ~ 75 ps) using a 375 nm excitation laser source. Details of the time resolved fluorescence setup have been discussed in our previous reports.[24,25] For the fluorescence anisotropy measurements, the emission polarizer was adjusted to be parallel and perpendicular to that of the excitation and the corresponding fluorescence transients are collected as I_{para} and I_{per}, respectively. The time-resolved anisotropy is defined as $r(t) = \dfrac{(I_{para} - G \times I_{per})}{(I_{para} + 2 \times G \times I_{per})}$. The magnitude of G, the grating factor of the emission monochromator of the TCSPC system, was found using a long tail matching technique. Time-resolved emission spectra (TRES) and time-resolved area normalized emission spectra (TRANES) were constructed following the methods described earlier[26,27] to determine the time dependent fluorescence Stokes shifts. In brief, the normalized spectral shift correlation function or the solvent correlation function, $C(t)$, is defined as $C(t) = \dfrac{\nu(t) - \nu(\infty)}{\nu(0) - \nu(\infty)}$, where $\nu(0)$, $\nu(t)$, and $\nu(\infty)$ are the emission peak maxima (in cm^{-1}) at time 0, t, and ∞ respectively.

The structure of the dye, ACYMAN, was built using the molecular builder interface of HyperChem 8.0 (Hypercube, Gainesville, FL, USA). The molecule was then optimized initially in vacuo at the ground state and also in its first excited state using the RM1 method utilizing the minimization protocol implemented in HyperChem 8.0.

12238 | Phys. Chem. Chem. Phys., 2017, **19**, 12237–12245

This journal is © the Owner Societies 2017

3. Results and discussion

3.1. Steady-state spectroscopic studies

ACYMAN is known to display strong polarity sensitive fluorescence. For example, the steady state emission peak maximum of the dye is significantly red shifted from 427 nm in cyclohexane to 517 nm in water.[19] This is attributed to a highly polar excited state originating from an intramolecular charge transfer (ICT) process, which is corroborated by theoretical calculations. Upon photoexcitation, the dipole moment of ACYMAN is found to change *in vacuo* from 2.0 D in the ground state to 7.1 D in the excited state, whereas, in ethanol it is found to be 4.03 D and 9.30 D, respectively, in the ground and excited states. Such a moderate change in dipole moment ($\Delta\mu \sim 5$ D) upon photoexcitation is the signature of an intramolecular charge transfer (ICT) process rather than a twisted intramolecular charge transfer (TICT), where usually a large change in dipole moment (~ 16 D) of the fluorophore is involved.[26] Fig. 1(a) shows the steady-state fluorescence spectra of the dye in DMF, aqueous buffer and 100 mM SDS solution (micelles). The emission maximum and quantum yield of the dye in DMF (455 nm and 0.53, respectively) compared to those in aqueous buffer (517 nm and 0.09, respectively) indicate stabilization of the ICT state in polar solvent. In comparison to DMF, the steady state emission peak maximum is significantly red shifted (~ 50 nm) to 502 nm in the anionic SDS micelles. The significant red shift

in the position of the emission peak maximum of ACYMAN in the SDS micelles compared to DMF and its moderate blue shift compared to aqueous buffer reveal the location of the dye at the water–head-group interface of the micelle. Furthermore, the similarity in the position of the steady state emission peak maximum of ACYMAN in the SDS micelles to that in methanol ($\lambda_{em.} \sim 497$ nm) (data not shown) is also consistent with the fact that the dye resides in the Stern layer of the anionic micelles, which is moderately polar and hydrogen bond donating.[27]

The steady state fluorescence spectrum of ACYMAN in the Histone-1 (H1) protein (110 μM) is similar to that in aqueous buffer (inset, Fig. 1(b)) indicating the absence of any interaction between the protein and the dye. Upon the addition of SDS (430 μM), a marked blue shift (~ 35 nm) in the steady state fluorescence spectrum of the dye in the H1-protein is observed, along with a significant increase in emission intensity. The blue shifted emission spectrum of ACYMAN at 485 nm compared to those in the protein (517 nm) and 430 μM SDS (517 nm, data not shown) solutions clearly indicates that the local environment around the dye significantly changed (lower polarity) in the protein–surfactant complex. It is well known that the anionic SDS surfactants strongly interact with the cationic nucleic protein H1 leading to the formation of a protein–surfactant interface.[21] Our observation indicates that binding of the SDS molecules to the protein (H1) reduces the number of water molecules accessible to the protein surface, resulting in a decrease of the local polarity of the protein–surfactant interface in comparison to the protein–water interface (Fig. 1(b)). Furthermore, the binding constant for ACYMAN to the host protein–SDS interface has been estimated to be 7.51×10^3 M^{-1} following the Benesi Hildebrand plot[28] as shown in the inset of Fig. 2(a). From this binding constant data, we have estimated that essentially all the dye molecules would remain bound to the protein–surfactant complex considering the concentrations of the dye and complex (equal to the concentration of the protein) to be 1 μM and 110 μM, respectively.

It is known that following the formation of the protein–surfactant complex upon addition of SDS to the H1 protein solution, significant structural change in the protein is induced,[29] especially in the N-terminal domain, which likely modifies the interface of the protein–surfactant complex compared to that of the protein. Both the CD-spectra and the fluorescence spectra of the single tyrosine (Tyr 72) residue of the H1-protein confirm such structural transition of the protein induced by SDS (Fig. 2(a) and (b)). As shown in Fig. 2(a) a significant ellipticity in the whole protein is induced in the complex, which is consistent with an increase in the α-helix content of the protein.[20,21] Moreover, a large enhancement of the fluorescence emission of the single tyrosine residue (Tyr 72) of the protein at 305 nm is observed upon addition of SDS and was ascribed to the transfer of Tyr 72 to a more hydrophobic environment.[30] As the H1 protein is known[20,29,31] to comprise a central globular domain flanked by a short amino-terminal domain (NTD) and a long carboxyl-terminal domain (CTD), anionic SDS causes electrostatic charge compensation of the positively charged lysine residues in the NTD and CTD through electrostatic interactions
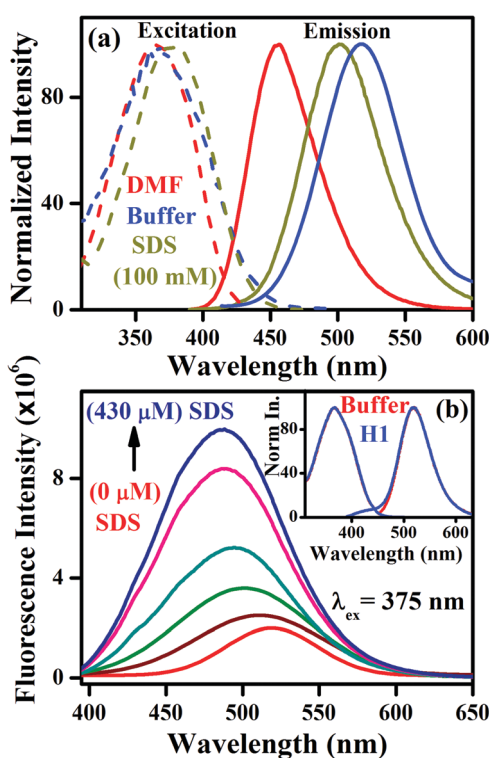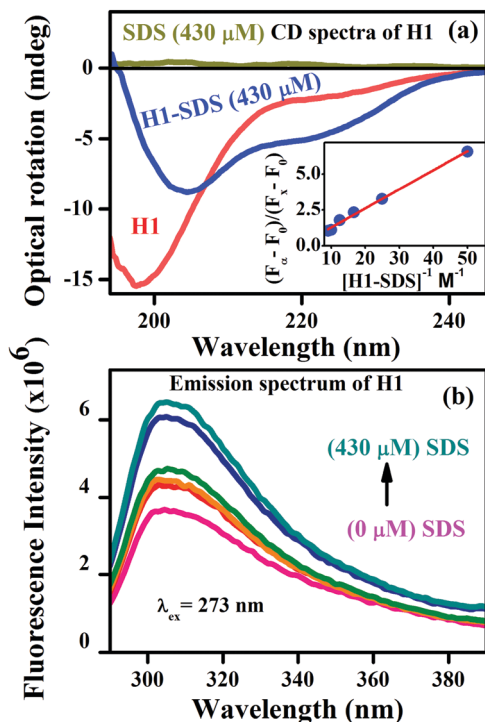

Fig. 1 (a) Steady state excitation and emission spectra of ACYMAN in various solvents and in the presence of SDS micelles (100 mM). (b) Fluorescence emission spectra of ACYMAN in H1 (110 μM) with increasing concentrations of SDS: inset shows excitation and emission spectra in H1 and aqueous buffer.

This journal is © the Owner Societies 2017

Phys. Chem. Chem. Phys., 2017, **19**, 12237–12245 | **12239**

Fig. 2 (a) Far UV-CD (circular dichroism) spectra of H1 (110 μM), SDS (430 μM) and the H1–SDS (430 μM) complex. Binding constant for ACYMAN to the H1–SDS interface is shown in the inset. (b) Effect of SDS on the fluorescence emission of H1.

Fig. 3 (a) Picosecond-resolved fluorescence transients of ACYMAN in aqueous buffer (χ^2 = 1.03) and SDS micelles (100 mM) (χ^2 = 1.07). (b) Picosecond-resolved fluorescence transients of ACYMAN in H1 (110 μM) (χ^2 = 1.09) and H1–SDS (430 μM) complex (χ^2 = 1.05).

and leads to folding of these positively charged domains *via* hydrophobic interactions.[24] In consequence, the Tyr 72 residue likely buries itself in a more hydrophobic region of the central globular domain of the protein resulting in significantly enhanced fluorescence intensity as shown in Fig. 2(b).

3.2. Time-resolved studies: dye-micelles (SDS)/protein (H1) interactions

Time-resolved fluorescence decay of ACYMAN in aqueous buffer (Fig. 3(a)) is characterized by a bi-exponential decay with a faster component of 0.27 ns (78%) and a longer component of 0.6 ns (22%) (Table 1). Such bi-exponential decay of the probe in a homogeneous medium like aqueous buffer is also observed for several fluorescent dyes including some coumarins,[32–35] and does not imply partitioning of the probe in two different environments.[33,36,37] This is indicative of the presence of different channels of radiative and non-radiative relaxation processes of the dye in polar solvents.[32] Following photoexcitation, ACYMAN is promoted to the locally excited state (LE) which is rapidly transferred to the intramolecular charge-transferred state (ICT) in polar solvents *via* ultrafast solvation and intramolecular charge transfer.[18,32] This ICT state of ACYMAN undergoes rapid non-radiative relaxation in water which gives rise to faster decay (~270 ps) with a major contribution (78%). The longer component of ~600 ps may be attributed to the lifetime of the ICT state in water. For the H1-protein, the fluorescence decay of the probe is very similar to that in aqueous buffer being characterized by two decay components identical to those
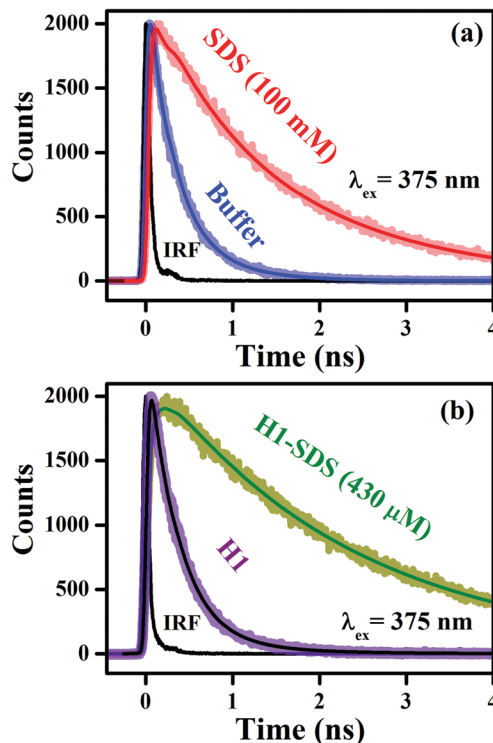
Table 1 Fluorescence lifetimes of ACYMAN in different systems

System/wavelength (nm)	τ_1 ns [%]	τ_2 ns [%]	τ_3 ns [%]
Aqueous buffer/517 nm	0.27 (78)	0.59 (22)	—
H1 (110 μM)/517 nm	0.28 (80)	0.63 (20)	—
SDS micelles (100 mM)/450 nm	0.025 (76)	0.24 (18)	1.55 (6)
SDS micelles (100 mM)/500 nm	0.032 (38)	0.74 (18)	1.78 (44)
SDS micelles (100 mM)/550 nm	0.25 (−11)	1.29 (59)	2.31 (30)
H1–SDS (430 μM)/430 nm	0.116 (48)	0.76 (37)	2.34 (15)
H1–SDS (430 μM)/480 nm	0.030 (−2)	1.10 (31)	2.37 (67)
H1–SDS (430 μM)/520 nm	0.050 (−19)	0.12 (15)	2.48 (66)

For various systems, the wavelengths (nm) of time-resolved decay measurements are shown. The amplitudes corresponding to the relevant decay components are shown within the parentheses.

in aqueous buffer, which excludes the possibility of any interaction between the probe and the host protein (Fig. 3(b)). Unlike aqueous buffer and protein (H1), the fluorescence decay components and their relative amplitudes vary continuously in going from the blue edge to the red edge of the emission spectra and the faster component at the blue end becomes a rise at the red end for the SDS micelles and the H1/SDS complex (Table 1). This is a manifestation of the solvation dynamics in the SDS micelles as well as in the protein–surfactant complex as discussed later.[38] The fluorescence decays of ACYMAN in SDS micelles and the H1–SDS complex at their corresponding emission maxima are shown in Fig. 3(a) and (b), respectively. It has to be noted that the one extra long component of fluorescence lifetime has been observed in SDS micelles as well as in the
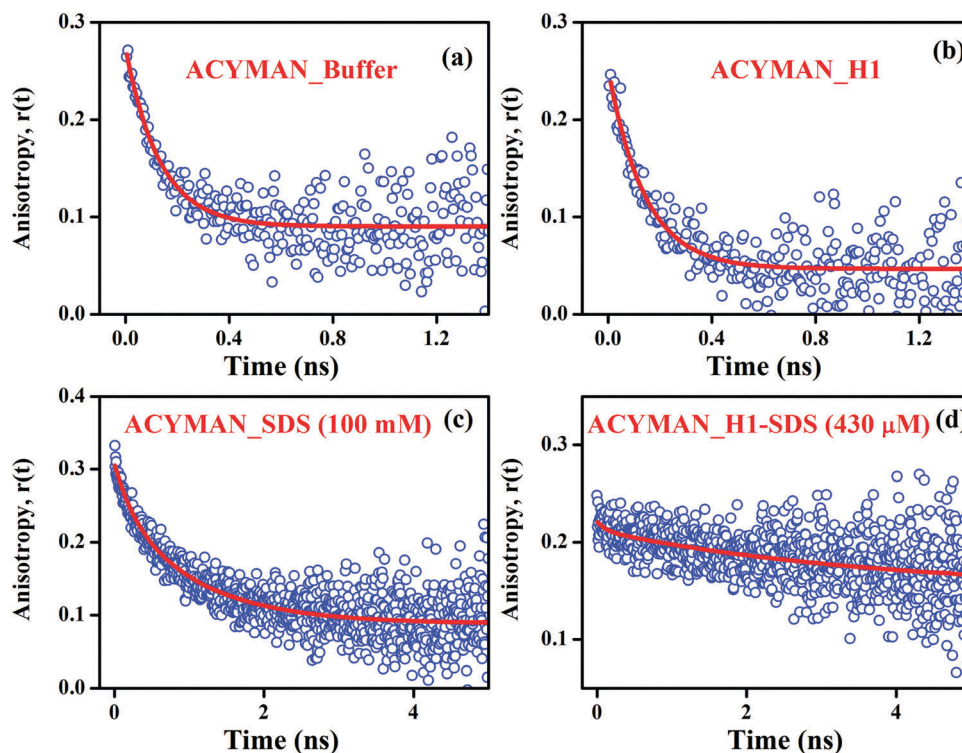
Fig. 4 Temporal decay of fluorescence anisotropy, $r(t)$, of ACYMAN in (a) aqueous buffer (χ^2 = 1.10), (b) H1 (110 μM) (χ^2 = 1.2), (c) SDS micelles (100 mM) (χ^2 = 1.5) and (d) the H1–SDS (430 μM) complex (χ^2 = 1.0).

H1–SDS complex compared to the aqueous buffer and H1 protein systems, while the contribution of the shorter component of the fluorescence life time in SDS micelles and the H1–SDS complex decreased significantly with respect to aqueous buffer and the H1 protein. To better assess the interactions of the probe with the hosts (SDS/H1) time-resolved fluorescence anisotropy decay, $r(t)$, measurements were carried out. For aqueous buffer (Fig. 4(a)) and the protein (H1) (Fig. 4(b)), the anisotropy decays are mono-exponential with similar rotational correlation times (Table 2), indicating the absence of any interaction between the probe ACYMAN and the H1-protein. The time-resolved anisotropy decay, $r(t)$, of ACYMAN is bi-exponential in the SDS micelles and in the H1-protein in the presence of SDS (430 μM), and can be described by eqn (1) in accordance with the "two-step" in combination with the "wobbling-in-cone" model.[39]

$$r(t) = \left(1 - S^2\right) \cdot \exp\left(-\frac{t}{\phi_1}\right) + S^2 \cdot \exp\left(-\frac{t}{\phi_2}\right) \quad (1)$$

where ϕ_1 and ϕ_2 are the fast and the slow rotational correlation times, respectively. S is the generalized order parameter related to the semi-cone angle θ_0 by eqn (2) as follows.

$$S = 0.5 \cos\theta_0(1 + \cos\theta_0) \quad (2)$$

For the SDS micelles, the anisotropy decay is significantly retarded compared to aqueous buffer (Table 2) and is characterized by two rotational time constants of 250 ps (23%) and 1.03 ns (77%), indicating strong interaction of the probe with the micelles (Fig. 4(c)). In accordance with the two-step model

Table 2 Time-resolved anisotropy parameters of ACYMAN in different systems

System	ϕ_1 ns [%]	ϕ_2 ns [%]	S	θ_0
Aqueous buffer	0.13 (100)	—		
SDS micelles (100 mM)	0.25 (23)	1.03 (77)	0.88	23.07
H1 (110 μM)	0.14 (100)	—		
H1–SDS (430 μM)	0.53 (12)	4.80 (88)	0.94	16.26

ϕ_1 and ϕ_2 are the rotational correlation times with their corresponding amplitudes shown within parentheses. S is the order parameter and θ_0 is the semicone angle in the wobbling-in-cone model.[39]

in combination with the wobbling-in-cone model, the shorter time constant of 250 ps may be attributed to the local motion of the probe within the micelle, whereas, the longer constant corresponds to the global tumbling motion of the entire micelle. The marked difference of the rotational time constants of the probe from aqueous buffer ($\sim$130 ps) corresponds to significant restriction of the orientational motion of the dye in the stern layer at the micelle–water interface. Time-resolved anisotropy decay of the probe in the H1-protein becomes remarkably slow (Fig. 4(d)) upon the addition of SDS (430 μM) (Table 2) indicating strong interaction of the ACYMAN probe with the H1-protein in the presence of SDS monomers. The time constants of 530 ps (12%) and 4.8 ns (88%) are consistent with the restricted local motion of the probe in the protein–surfactant interface and the global tumbling motion of the protein–surfactant complex, respectively. The generalized order parameter, S, which provides information about the packing[36] in the vicinity of the probe molecule is remarkably high for both SDS micelles (0.88)

and the H1–SDS complex (0.94) and is consistent with the location of the probe at the micelle–water interface and the protein–surfactant interface, respectively. Furthermore, a higher value of S and a lower value of the semi-cone angle θ_0 for the H1–SDS complex compared to the SDS micelles indicate greater restriction of the orientational motion of the probe at the protein–surfactant interface than at the micelle–water interface. This is consistent with the presence of a more highly rigid layer of water molecules at the protein–surfactant interface than at the micelle–water interface.

3.3. Dynamics of solvation at different interfaces

Fig. 5(a) and 6(a) show the wavelength-dependent emission transients of ACYMAN in SDS micelles and in the H1/SDS complex at three characteristic wavelengths, from the blue end to the
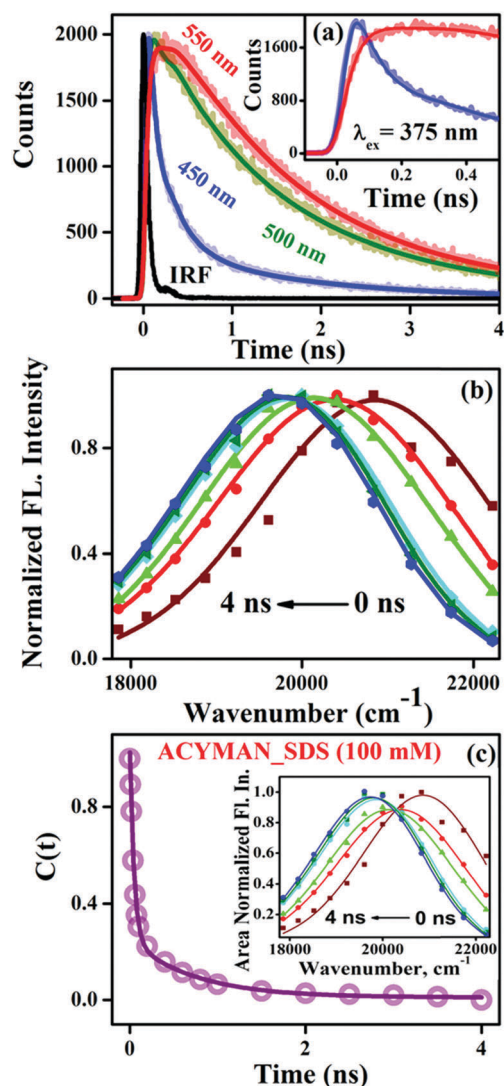

Fig. 5 (a) Picosecond-resolved emission transients of ACYMAN in SDS micelles (100 mM) at 450 nm (χ^2 = 1.1), 500 nm (χ^2 = 1.07) and 550 nm (χ^2 = 1.03). (b) Time-resolved emission spectra (TRES) of the corresponding systems are shown. (c) Decay of the solvation correlation function, $C(t)$, with time. Time-resolved area normalized emission spectra (TRANES) are shown in the inset.

Fig. 6 (a) Picosecond-resolved emission transients of ACYMAN in the H1–SDS (430 μM) complex at 430 nm (χ^2 = 1.06), 480 nm (χ^2 = 1.09) and 520 nm (χ^2 = 1.05). (b) Time-resolved emission spectra (TRES) of the corresponding systems are shown. (c) Decay of the solvation correlation function, $C(t)$, with time. Time-resolved area normalized emission spectra (TRANES) are shown in the inset.
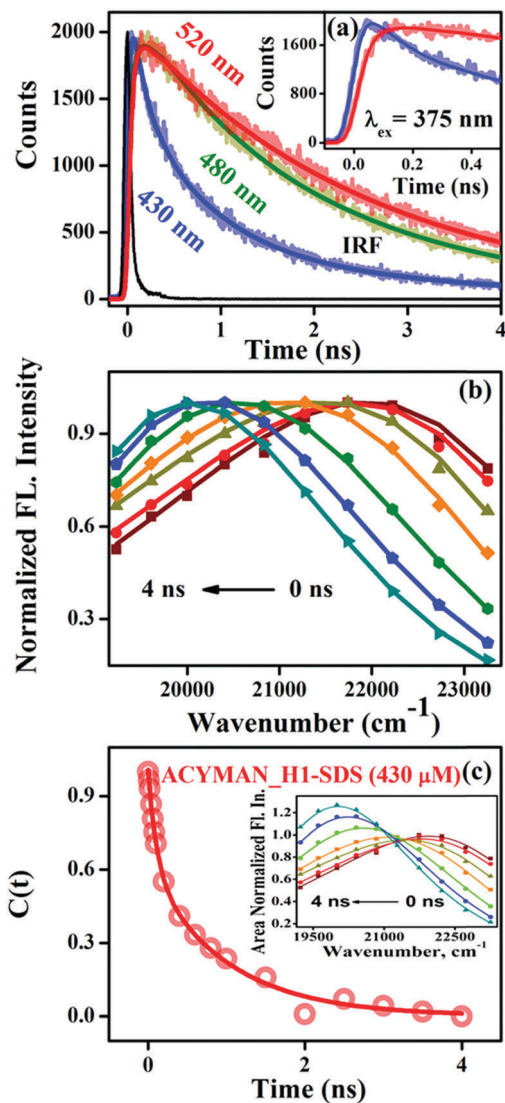
red end of the steady state fluorescence spectrum. The time-resolved fluorescence at the blue and the red end is characterized by a decay and a rise, respectively, indicating reorganization of the surrounding water molecules around the excited state dipole of the fluorophore which is manifested as the time-dependent shift of the fluorescence spectrum to the red end (Fig. 5(b) and 6(b)). The heterogeneity of the environments around the probe in the micelle and in the protein–surfactant complex is ruled out as no iso-emissive points in the time resolved area normalized emission spectra (TRANES)[40] are observed as shown in the insets of Fig. 5(c) and 6(c).

For the SDS micelles, the solvation correlation function, $C(t)$, decays (Fig. 5(c)) with two time constants of 50 ps (76%) and 800 ps (24%), indicating mediation of two types of water

12242 | Phys. Chem. Chem. Phys., 2017, 19, 12237–12245

This journal is © the Owner Societies 2017

trajectories in the solvent relaxation in the micelle–water interface. Similar bimodality with time constants of 140 ps (77%) and 2.14 ns (23%) was observed by other studies on the solvation dynamics of various fluorescent probes in anionic SDS micelles.[41,42] In accordance with Zewail et al.[43] the faster component (50 ps) may be attributed to the micelle surface-bound water molecules, whereas, the slower component of a few hundreds of picoseconds (800 ps) reflects coupling of the internal motion of the surfactant molecules with the water molecules of the Stern layer.[44] In sharp contrast to the micelles, the picosecond-resolved emission transients of ACYMAN in the H1-protein monitored at the blue and red end of the fluorescence spectrum are more or less similar (data not shown) and no rise is observed in the emission transient at the red end. This observation is consistent with very fast solvation of ACYMAN in the protein–water interface due to bulk type water molecules similar to the observations of Zewail et al.[18] In consequence no rise component associated with solvent relaxation could be detected in our TCSPC set up with a time resolution of 20 ps. The emission transients of the probe in the H1-protein become dramatically different (Fig. 6(a)) upon interaction with SDS. The solvation correlation function, $C(t)$, for the H1–SDS interface is characterized by two time constants, 110 ps (40%) and 1.0 ns (60%). This bimodal solvation dynamics in the H1–SDS interface indicates significant contributions of the surface-bound water molecules and structural fluctuation of the protein–surfactant complex in contrast to the significant role of the bulk type water molecules in the solvation dynamics at the protein (H1)–water interface.

Subtle but distinct differences between the micelle–water and protein–surfactant interfaces are noted, warranting further discussion. First of all, the faster component of solvation (τ_1) increases more than two-fold on going from the Stern layer of the SDS micelles to the protein–surfactant interface of the H1–SDS complex (Table 3). In addition, there is a significant increase (from 24% to 60%) in the contribution of the slower component (τ_2) as well as its magnitude. The two-fold increase in the faster component may be ascribed to the exertion of a stronger electrostatic field on the water molecules at the protein–surfactant interface than at the micelle–water interface. The binding surface of the H1-protein is positively charged due to the presence of a large number of positively charged residues in its N- and C-terminal domains, whereas the surfactant (SDS) is negatively charged owing to the presence of a negatively charged sulfate head group. As the anionic surfactants anchor to the positively charged lysine residues on the terminal domains of the protein, mutual electrostatic interaction between them gives rise to a strong electrostatic field[35] that significantly slows down the dynamics of the interfacial water at the protein–surfactant interface compared to the micelle–water interface. In addition, due to the anchoring of the negatively charged surfactant

molecules on the positively charged surface of the H1 protein, the hydrophobicity of the lysine side-chains increases as a result of electrostatic charge compensation followed by folding of the CTD and NTD in the H1–SDS complex.[20,29] This in turn likely induces a crowded environment of the lysine side-chains and the surfactant molecules anchored to the surface of the protein, which imposes significant restriction on the structural fluctuation of the surfactant molecules in the H1–SDS complex compared to the SDS micelles. In consequence, the contribution of the slower solvation component (τ_2) increases significantly along with its magnitude on going from the Stern layer of the SDS micelles to the protein–surfactant interface of the H1–SDS complex.

In order to compare the sensitivity of ACYMAN toward the biomolecular interfaces, some other non-covalent solvation probes, coumarin 500 (C500) and DCM were also used for the studies. The reason behind the choice of the two specific probes lies in the fact that C500 is a polar probe which is soluble in water and can be incorporated at the SDS micellar surface.[44] On the other hand DCM is hydrophobic and completely insoluble in water, however, it can also be incorporated at the same micellar surface.[45,46] The time scales of solvation dynamics obtained from these two probes at the micellar surface are found to be significantly different. While the reported average time constant of DCM solvation at the SDS micellar surface is 1.4 ns[46] the observed average time constant of C500 solvation is 0.07 ns (Fig. 7a). The difference of the local environments around the
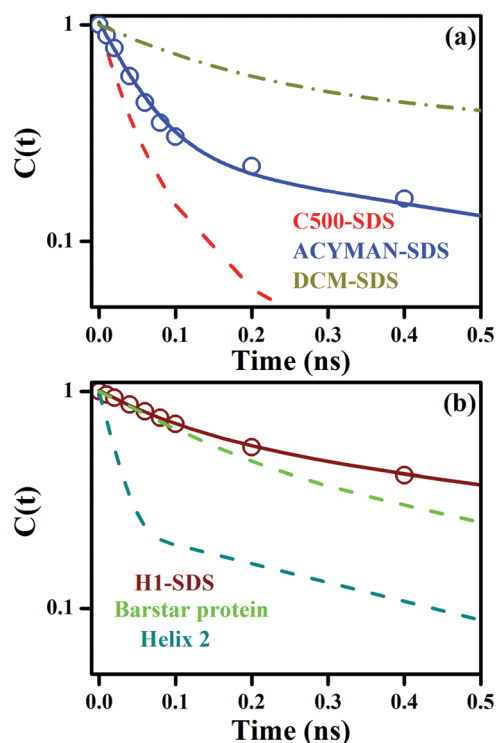

Fig. 7 (a) Solvation correlation function, $C(t)$, of C500, ACYMAN and DCM in SDS micelles (100 mM). (b) The decay of the solvation correlation function, $C(t)$, of the H1–SDS complex; the dotted line represents the $C(t)$ of α helix-2 and Barstar protein.

Table 3 Solvation correlation data for ACYMAN in different systems

System	τ_1 ns [%]	τ_2 ns [%]	τ_{avg} ns
SDS micelles (100 mM)	0.05 (76)	0.80 (24)	0.23
H1–SDS (430 μM)	0.11 (40)	1.00 (60)	0.64

This journal is © the Owner Societies 2017

Phys. Chem. Chem. Phys., 2017, 19, 12237–12245 | 12243

probes for the same micellar surface can easily be concluded from the time constants of solvation, because of the nature of the probes as discussed earlier. In other words, whereas C500 is more compatible to be localized on the polar side (head group region) of the micellar surface, DCM prefers to reside in the more hydrophobic portion of the surface of the micelles.[47] From Fig. 7(a) it is also clear that the time scale of solvation dynamics of ACYMAN lies between that of C500 and DCM. Thus it is interesting to note which of the above dyes is eligible to probe the interfacial solvation dynamics. We have observed that C500 reveals bulk water type solvation dynamics for the H1 protein, SDS below the critical micellar concentration (cmc) and the dynamics is also insensitive to the formation of the H1–SDS interface. On the other hand, the dye DCM remains insoluble in H1, SDS below the cmc and even at the protein–surfactant interface after the formation of the H1–SDS complex. In the case of ACYMAN, the dynamics of solvation is distinct in the H1–SDS interface from that in SDS below or above the cmc as described earlier.

A comparative study of the solvation dynamics of the interface after the formation of an α-helix in the H1 protein to that of the hydration dynamics of other α-helix proteins is evident in Fig. 7(b) in a time window of 500 ps. Molecular dynamics simulations on the α-helix containing protein shows that the dynamics of hydration in close proximity to the α-helix reveals ultrafast time components (75%) with a longer component of 500 ps (25%).[14,48] In another femtosecond resolved time-dependent dynamic stocks shift (TDSS) study on α-helix containing barstar protein, a slower component of 578 ps (59%) is manifested in the hydration dynamics.[49] The faster portion of the dynamics is concluded to be the rotational motion of the water molecules in close proximity to the α-helix. Thus slower components of hydration dynamics in the α-helix portion of different proteins are consistent with our studies.

Conclusions

Time-resolved fluorescence studies of a new, dipolar fluorophore 6-acetyl-(2-((4-hydroxycyclohexyl)(methyl)amino)naphthalene) (ACYMAN) unveils interesting features of solvation dynamics and local molecular dynamics in different interfaces of H1-protein, SDS micelles and H1–SDS complex. Time-resolved anisotropy decay of the dye is characterized by a time constant of ∼130–140 ps in aqueous buffer and protein, but the decay becomes slower in SDS micelles than in aqueous buffer or H1-protein, indicating stronger interaction of the dye with the micelles than the protein. Upon the addition of SDS surfactants, the anisotropy decay becomes significantly retarded in the H1–SDS interface compared to the SDS micelles, which indicates significantly stronger interaction of the dye with the H1–SDS complex than the micelles. Our studies also demonstrate that other well-known commercially available solvation dyes including C500 and DCM fail to probe the protein–surfactant interface of the H1–SDS complex. We have also compared the observed solvation dynamics of the interface with those from MD

simulations and femtosecond resolved studies reported in the literature. The observed time scale of solvation dynamics for ACYMAN is consistent with the slower components of the hydration dynamics as mentioned in the literature. This slower dynamics of ACYMAN likely originates from the structurally ordered water molecules (SOW) at the helix–surfactant interface.

References

1 W. Dubitzky, J. Southgate and H. Fuss, *Understanding the dynamics of biological systems: lessons learned from integrative systems biology*, Springer Science & Business Media, 2011.
2 J. A. Rupley and G. Careri, *Adv. Protein Chem.*, 1991, **41**, 37–172.
3 B. Halle, *Philos. Trans. R. Soc., B*, 2004, **359**, 1207–1224.
4 J.-M. Zanotti, G. Gibrat and M.-C. Bellissent-Funel, *Phys. Chem. Chem. Phys.*, 2008, **10**, 4865–4870.
5 R. Jimenez, G. R. Fleming, P. Kumar and M. Maroncelli, *Nature*, 1994, **369**, 471–473.
6 M. Maroncelli and G. R. Fleming, *J. Chem. Phys.*, 1987, **86**, 6221–6239.
7 N. Nandi, K. Bhattacharyya and B. Bagchi, *Chem. Rev.*, 2000, **100**, 2013–2046.
8 K. Bhattacharyya, *Acc. Chem. Res.*, 2003, **36**, 95–101.
9 A. H. Zewail, *Angew. Chem., Int. Ed.*, 2000, **39**, 2586–2631.
10 B. Born, H. Weingärtner, E. Bründermann and M. Havenith, *J. Am. Chem. Soc.*, 2009, **131**, 3752–3755.
11 S. K. Pal and A. H. Zewail, *Chem. Rev.*, 2004, **104**, 2099–2124.
12 E. Potter, J. Herek, S. Pedersen, Q. Liu and A. Zewail, *Nature*, 1992, **355**, 66–68.
13 S. Choudhury, S. Batabyal, P. K. Mondal, P. Singh, P. Lemmens and S. K. Pal, *Chem. – Eur. J.*, 2015, **21**, 16172–16177.
14 S. Bandyopadhyay, S. Chakraborty, S. Balasubramanian and B. Bagchi, *J. Am. Chem. Soc.*, 2005, **127**, 4071–4075.
15 D. R. Buckler, E. Haas and H. A. Scheraga, *Biochemistry*, 1995, **34**, 15965–15978.
16 E. M. Kirilova, I. Kalnina, T. Zvagule, N. Gabruseva, N. Kurjane and I. I. Solomenikova, *J. Fluoresc.*, 2011, **21**, 923–927.
17 R. W. Sinkeldam, N. J. Greco and Y. Tor, *Chem. Rev.*, 2010, **110**, 2579–2619.
18 D. Zhong, S. K. Pal and A. H. Zewail, *ChemPhysChem*, 2001, **2**, 219–227.
19 S. Singha, D. Kim, B. Roy, S. Sambasivan, H. Moon, A. S. Rao, J. Y. Kim, T. Joo, J. W. Park and Y. M. Rhee, *Chem. Sci.*, 2015, **6**, 4335–4342.

20 A. Roque, I. Ponte and P. Suau, *J. Phys. Chem. B*, 2009, **113**, 12061–12066.

21 S. Bathaie, A. Moosavi-Movahedi, B. Ranjbar and A. Saboury, *Colloids Surf., B*, 2003, **28**, 17–25.

22 J. Bednar, R. A. Horowitz, S. A. Grigoryev, L. M. Carruthers, J. C. Hansen, A. J. Koster and C. L. Woodcock, *Proc. Natl. Acad. Sci. U. S. A.*, 1998, **95**, 14173–14178.

23 J. R. Errington and P. G. Debenedetti, *Nature*, 2001, **409**, 318–321.

24 S. Choudhury, S. Batabyal, T. Mondol, D. Sao, P. Lemmens and S. K. Pal, *Chem. – Asian J.*, 2014, **9**, 1395–1402.

25 P. Singh, S. Choudhury, G. K. Chandra, P. Lemmens and S. K. Pal, *J. Photochem. Photobiol., B*, 2016, **157**, 105–112.

26 Z. R. Grabowski, K. Rotkiewicz and W. Rettig, *Chem. Rev.*, 2003, **103**, 3899–4032.

27 E. Fuguet, C. Ràfols, E. Bosch and M. Rosés, *Langmuir*, 2003, **19**, 55–62.

28 A. Mallick, B. Haldar and N. Chattopadhyay, *J. Phys. Chem. B*, 2005, **109**, 14683–14690.

29 A. Roque, N. Teruel, R. López, I. Ponte and P. Suau, *J. Struct. Biol.*, 2012, **180**, 101–109.

30 J. G. Gavilanes, M. A. Lizarbe, A. M. Munico and M. Oñaderra, *Int. J. Pept. Protein Res.*, 1985, **26**, 187–194.

31 J. Allan, P. Hartman, C. Crane-Robinson and F. Aviles, *Nature*, 1980, **288**, 675–679.

32 J. Dana, T. Debnath, P. Maity and H. N. Ghosh, *J. Phys. Chem. C*, 2015, **119**, 2046–2052.

33 A. Chatterjee and D. Seth, *Photochem. Photobiol.*, 2013, **89**, 280–293.

34 A. Chatterjee, B. Maity and D. Seth, *Phys. Chem. Chem. Phys.*, 2013, **15**, 1894–1906.

35 P. Verma and H. Pal, *J. Phys. Chem. A*, 2012, **116**, 4473–4484.

36 A. Mishra, G. Behera, M. Krishna and N. Periasamy, *J. Lumin.*, 2001, **92**, 175–188.

37 G. Saroja, B. Ramachandram, S. Saha and A. Samanta, *J. Phys. Chem. B*, 1999, **103**, 2906–2911.

38 E. Middelhoek, H. Zhang, J. Verhoeven and M. Glasbeek, *Chem. Phys.*, 1996, **211**, 489–497.

39 E. L. Quitevis, A. H. Marcus and M. D. Fayer, *J. Phys. Chem.*, 1993, **97**, 5762.

40 A. Koti, M. Krishna and N. Periasamy, *J. Phys. Chem. A*, 2001, **105**, 1767–1771.

41 Y. Tamoto, H. Segawa and H. Shirota, *Langmuir*, 2005, **21**, 3757–3764.

42 N. Nandi, K. Bhattacharyya and B. Bagchi, *Chem. Rev.*, 2000, **100**, 2013–2046.

43 L. Zhao, S. K. Pal, T. Xia and A. H. Zewail, *Angew. Chem., Int. Ed.*, 2004, **43**, 60–63.

44 S. Choudhury, P. K. Mondal, V. Sharma, S. Mitra, V. G. Sakai, R. Mukhopadhyay and S. K. Pal, *J. Phys. Chem. B*, 2015, **119**, 10849–10857.

45 R. Sarkar, A. K. Shaw, M. Ghosh and S. K. Pal, *J. Photochem. Photobiol., B*, 2006, **83**, 213–222.

46 S. K. Pal, D. Sukul, D. Mandal, S. Sen and K. Bhattacharyya, *Chem. Phys. Lett.*, 2000, **327**, 91–96.

47 S. K. Pal, D. Sukul, D. Mandal and K. Bhattacharyya, *J. Phys. Chem. B*, 2000, **104**, 4529–4531.

48 S. Bandyopadhyay, S. Chakraborty, S. Balasubramanian, S. Pal and B. Bagchi, *J. Phys. Chem. B*, 2004, **108**, 12608–12616.

49 A. Jha, K. Ishii, J. B. Udgaonkar, T. Tahara and G. Krishnamoorthy, *Biochemistry*, 2010, **50**, 397–408.